

# 1. Introduction

High energy resolution and angle-resolved electron spectroscopy is widely used to investigate various atomic processes (ionization, Auger decay, etc.). In the last 40 years several electrostatic electron spectrometers were developed at Atomki for studying ionization processes [2]; [3]; [4]; [5]; [6]; [7]. Two of them are special combination of a spherical and a cylindrical analyzer (marked as ESA-21 and ESA-22). Both of them were built for measuring simultaneously energy and angular distributions of electrons emitted from different collision systems [6]; [7]. These electron optical arrangements reduce the measuring time by more than a factor of ten relative to the earlier applied techniques [1]. However, the intensity calibration remains difficult. In this paper we present the results measured by the recently upgraded ESA-22 electrostatic electron spectrometer. The aim of this development was to reduce the difficulty of the intensity calibration independently from the kinetic energy of the electrons ejected from the collision region. A new calibration method has been developed which does not use any data published in the literature for determination of the relative detector efficiencies and the spectrometer transmission. In the present work elastic electron scattering process was applied for calibration. Argon gas target was bombarded with electrons of the kinetic energy of 205 eV.

## 2. The upgraded ESA-22 spectrometer

The ESA-22 electrostatic electron analyzer (Fig. 1) is a modified version of the ESA-21 [6]. Both of them consist of a spherical mirror analyzer (SMA) and a cylindrical mirror analyzer (CMA). The SMA focuses the electrons from the scattering plane to the entrance slit of the CMA performing the energy analysis of the electrons. The main difference between the two spectrometers is the construction of the CMA. The ESA-21 has a double pass ring-point-ring focusing analyzer while the ESA-22 has a single pass ring-ring focusing electrode system. Both spectrometers are characterized by second order focusing property. When position sensitive detectors, e.g. channel plates are applied in the ESA-22 the electrons are focused to either 20 mm or 70 mm diameters. An additional possibility is to use 24 channel electron multipliers (CEMs) at 90 mm focal diameter. In the present paper we employ CEMs for the calibration. Furthermore, the outer sphere and cylinder are cut into two halves resulting that the system is capable of measuring the angular distribution of electrons at two independent energies simultaneously in the polar angular ( $\psi$ ) range of  $\pm 15^\circ$  and  $\pm 165^\circ$  relative to the beam direction (see Fig. 2a). This is achieved by applying different voltages on the outer sphere and cylinder parts. In the cutting plane field correction electrodes are positioned to reach near-ideal electrical fields for the half spectrometers.

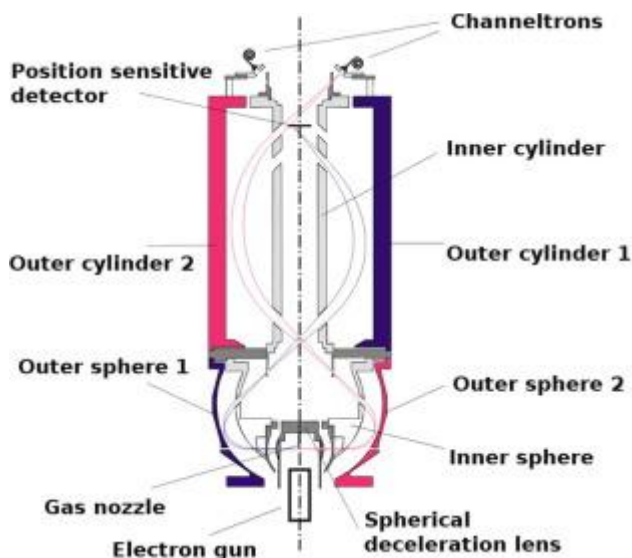


Fig. 1.

Schematic cross section of the upgraded ESA-22 electron spectrometer.

[Figure options](#)

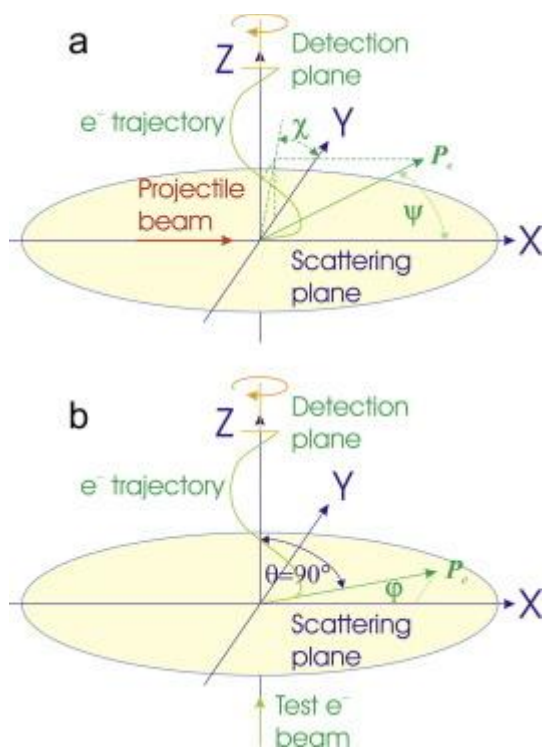


Fig. 2.

Measuring geometry (a) in case of the incident beam directed towards the  $X$  axis and (b) using the electron gun placed along the spectrometer axis ( $Z$  axis) as excitation source.  $P_e$  denotes the momentum of the emitted electrons.

[Figure options](#)

The two detector systems can be employed parallel. The electrons in one half of the spectrometer can be focused to a 20 mm diameter ring while in the other half to a 90 mm diameter ring. According to this arrangement (see [Fig. 1](#)) the ESA-22 analyzer can be applied for electron–

electron coincident experiments, as well [7]. A spherical deceleration lens is placed around the source region to improve the energy resolution of the system. The relative energy resolution is better than  $2.8 \times 10^{-3}$  without deceleration.

New UHV chamber, magnetic shielding and a special detector holder were designed and built. The analyzer and the interaction region are shielded from the Earth's magnetic field by one layer (3 mm thick) of  $\mu$ -metal sheet. The residual magnetic field in the scattering plane and in the analyzer is less than 5 mG. The new vacuum chamber and the detector holder are continuously rotatable under UHV conditions around the beam direction ( $X$  axis in Fig. 2a) and the spectrometer axis ( $Z$  axis in Fig. 2), respectively. The rotation of the vacuum chamber enables to observe the electrons emitted from the target region at different emission planes, i.e. at different azimuthal emission angles ( $\chi$ ) and 3D angular distribution can be measured (see Fig. 2a). By rotating the detector holder the relative efficiencies of the individual detectors and the angle dependent transmission function of the analyzer can be easily determined at arbitrary electron energies. 24 new channeltrons (CEMs) are mounted on the holder at every  $15^\circ$ . The angular window of each CEM is  $\pm 1.7^\circ$  in vertical and  $\pm 3.5^\circ$  in horizontal direction. In the present calibration experiment the polar angle was constant and perpendicular ( $\theta = 90^\circ \pm 1.7^\circ$ ) to the incoming electron beam and the angular distributions were measured as a function of the azimuth angle ( $\varphi$  in Fig. 2b). An electron gun along the spectrometer axis was installed (see Figs. 1 and 2b) which makes calibration possible at arbitrary electron energies using elastic and inelastic electron scattering processes. New software has been also developed in LabView to control the voltages on the electrodes of the spectrometer, the rotation of the detector holder as well as the data collection.

### 3. The relative calibration method

Different calibration methods exist in electron spectroscopy. In case of the absolute method all parameters (gas density, beam current, etc.) included in Eq. (1) are determined independently [8]. For relative calibration known cross sections are used to determine the measured unknown cross sections. In our photoelectron angular distribution experiments [9]; [10]; [11] the second method were applied for the determination of the detector efficiencies and spectrometer transmission by using the LMM Auger lines of argon. The experimental single differential cross section can be expressed in the following way:

equation(1)

$$\frac{d\sigma}{d\Omega} = \frac{I_d}{I_p n_t L T \eta \Delta\Omega},$$

[Turn MathJax on](#)

where  $I_d$  and  $I_p$  are the number of the detected electrons and the incident particles, respectively.  $n_t$  indicates the density of the target [ $atom/cm^3$ ],  $L$  is the target thickness [ $cm$ ] in the direction of the projectile beam and  $\eta$  is the detection efficiency of the individual CEMs.  $T$  denotes the transmission of the spectrometer, while  $\Delta\Omega$  represents the solid angle [ $sr$ ].  $I_p$  can be obtained from the current recorded with a Faraday cup. The target density ( $n_t$ ) for gas target can be measured with an absolute pressure gauge and  $L$  can be determined from an isotropic process (e.g. in our case the

$L_{23}M_{23}M_{23}$  Auger group was measured at 2 MeV proton and 1.9 keV electron impacts).  $\Delta\Omega$  is known from the geometry of the analyzer (from the slit size of the inner sphere and the open area of the channeltrons) and its value is  $4.7(2)\times 10^{-3}$  sr (error in the brackets) for a single angular channel.

The transmission ( $T$ ) is unity for an ideal spectrometer but not for a realistic electrostatic system. Its determination is difficult due to the lens effect at the slits of the inner sphere and cylinder, the residual magnetic field, the inhomogeneity in the conductivity of the electrodes surfaces, etc. Furthermore, the detector efficiencies also differ from each other due to the manufacturing procedure and the surface contamination (different vacuum conditions). The efficiency may change with the elapsed time as well. In the present calibration method the transmission of the spectrometer and the efficiencies of the detectors were experimentally determined using elastically scattered electrons on Ar target at 205 eV impact energy. The diameter of the electron beam is 0.6 mm at the target region. In this case only those electrons are detected which are emitted at polar angle  $\theta=90^\circ$  relative to the momentum of the incident electron beam (see Fig. 2b). This means that the differential emission cross sections are the same for all observation angles ( $\varphi$  in Fig. 2b) due to the cylindrical symmetry of the collision process. It is true for both the elastic and the inelastic scattering processes. If the intensities detected with different detectors are not identical as a function of the observation angle ( $\varphi$  in Fig. 2b), it indicates that either the transmission of the spectrometer or the detector efficiencies differ from the ideal case. In order to find the origin of these differences the detector holder was rotated around the symmetry axis of the spectrometer ( $Z$  axis in Fig. 2). The electron spectra were collected with every detector at every observation angle  $\varphi$  between  $\pm 15^\circ$  and  $\pm 165^\circ$  in  $15^\circ$  steps relative to the  $X$  axis (see Fig. 2b). Fig. 3 demonstrates that the shapes of the measured angular distributions are similar for all channeltrons and only the numbers of counted electrons are different. If we assume that the efficiencies of the detectors were constant during the experiment (3 days) then the observed anisotropic angular distribution originate from the non-isotropic transmission of the analyzer. In order to estimate the transmission the average of the measured intensity ( $\langle I_i \rangle$ ) for the  $i$  th detector ( $i=1\dots 24$ ) can be calculated as:

equation(2)

$$\langle I_i \rangle = \frac{\sum_{j=1}^{23} I_i(\varphi_j)}{23},$$

[Turn MathJax on](#)

where  $I_i(\varphi_j)$  represents the intensity measured by the  $i$  th detector,  $\varphi_j = \varphi_{i0} + (j-1)\Delta\varphi$  is the angular position of the  $i$  th detector,  $\Delta\varphi$  denotes the angular step of the rotation ( $15^\circ$  in the present experiments) and  $\varphi_{i0}$  indicates the initial position of the individual detectors before rotation. Using this mean value the measured transmission of the  $i$  th detector ( $t_i(\varphi_j)$ ) is

equation(3)

$$t_i(\varphi_j) = \frac{I_i(\varphi_j)}{\langle I_i \rangle}.$$

[Turn MathJax on](#)

In this way a  $24 \times 23$  dimension transmission matrix was created. The averaged transmission ( $\langle T(\varphi_j) \rangle$ ) at detection angle  $\varphi_j$  is as follows:

equation(4)

$$\langle T(\varphi_j) \rangle = \frac{\sum_{i=1}^{24} t_i(\varphi_j)}{24}$$

[Turn MathJax on](#)

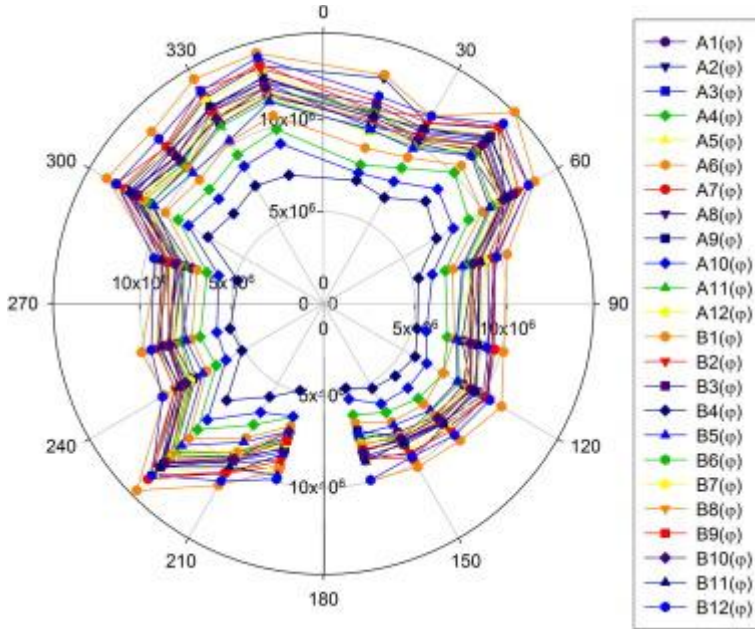


Fig. 3.

Raw intensity spectra as a function of the observation angle  $\varphi$  (in degree) in polar coordinate system (see Fig. 2b). The symbols connected with solid lines represent the elastic peak intensities of the individual detectors (denoted by A1-A12 and B1-B12). Each line shows a different detector positioned at different detection angle. The kinetic energy of the elastically scattered electrons was 205 eV.

[Figure options](#)

Fig. 4 shows the measured transmissions for all detectors as a function of the observation angle. They agree very well independently from the detector efficiencies. This good agreement confirms that the efficiencies of the detectors were stable during the experiment. Correcting the measured intensities with the mean transmission ( $\langle T(\varphi_j) \rangle$ ) we get isotropic angular distributions for all detectors but with different intensities (see Fig. 5). These differences can be interpreted as the different efficiencies of the detectors. To determine the detector efficiencies we can derive an angle independent mean value ( $\langle I_i^T \rangle$ ) for the  $i$  th detector from the transmission corrected intensities ( $I_i^T(\varphi_j)$ ) where  $\varphi_j$  is the detection angle):

equation(5)

$$\langle I_i^T \rangle = \frac{\sum_{j=1}^{23} I_i^T(\varphi_j)}{23}$$

[Turn MathJax on](#)

Now a detector independent intensity can be calculated

equation(6)

$$\langle I \rangle = \frac{\sum_{i=1}^{24} I_i^T}{24}.$$

[Turn MathJax on](#)

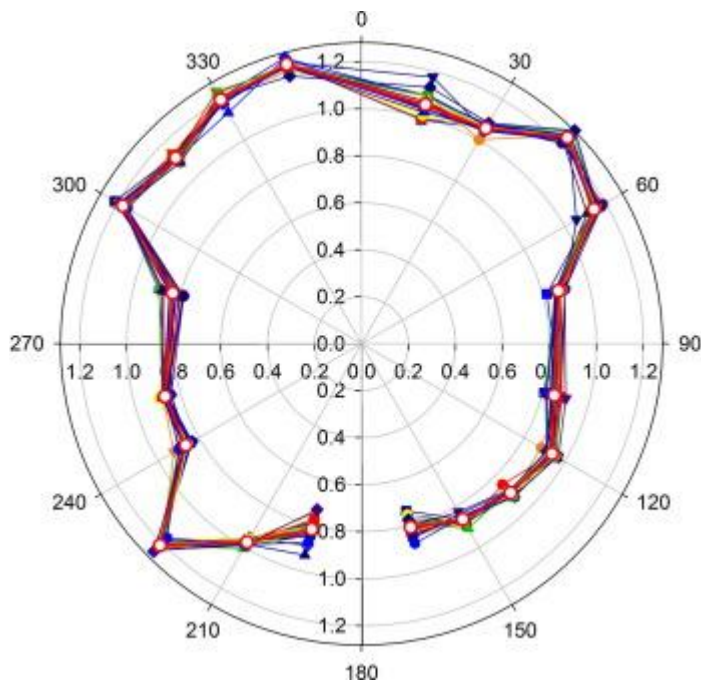


Fig. 4.

Transmissions  $t_i(\varphi_j)$  measured with individual detectors (symbols connected with solid lines) and their mean values (red open circles connected with thick red line). The symbols, lines and colors correspond to the ones in Fig. 3. The kinetic energy of the elastically scattered electrons was 205 eV. (For interpretation of the references to colour in this figure legend, the reader is referred to the web version of this article.)

[Figure options](#)

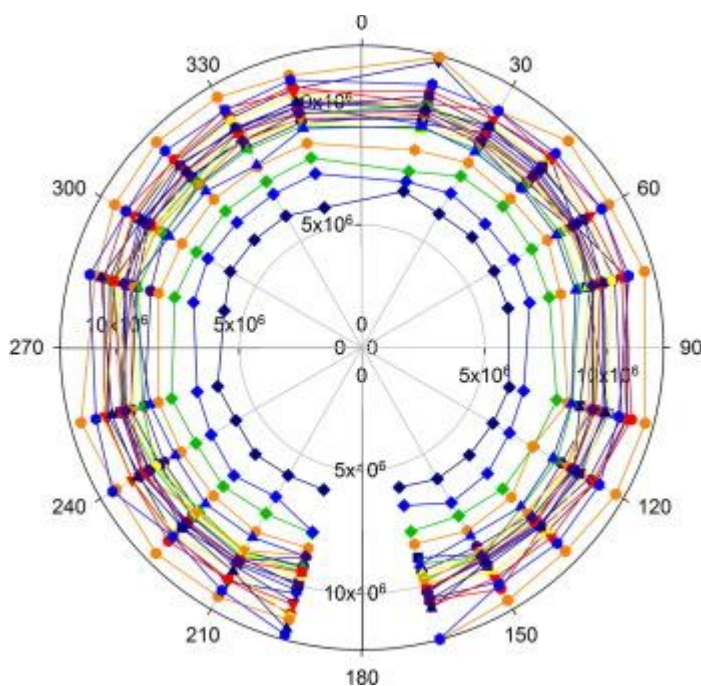


Fig. 5.

Transmission corrected peak intensities as a function of the detection angle. The symbols, lines and colors correspond to the ones in [Fig. 3](#). The kinetic energy of the elastically scattered electrons was 205 eV. (For interpretation of the references to colour in this figure legend, the reader is referred to the web version of this article.)

### [Figure options](#)

The relative efficiencies for the  $i$  th detectors ( $\eta_i$ ) can be written as

equation(7)

$$\eta_i = \frac{\langle I_i^T \rangle}{\langle I \rangle}.$$

### [Turn MathJax on](#)

Using this procedure the transmission function of the spectrometer ([Fig. 4](#)) and the relative efficiencies of the detectors ([Fig. 6](#)) can be determined by means of the elastic scattering process at arbitrary electron energy without any data from the literature. In order to check the tilt angle between the electron beam direction and the scattering plane, similar experiment was performed for the inelastic process of Ar  $L_{23}M_{23}M_{23}$  Auger group (its average energy is also 205 eV) excited by 1.9 keV electrons. Both the spectrometer transmission function and the detector efficiencies calculated with the above mentioned method agree with the results obtained for the elastic scattering process. This means there is no tilt angle problem between the scattering plane and the electron beam direction, i.e. the polar angle  $\theta$  is  $90^\circ$  (see [Fig. 2b](#)). Since the transmission function of an electrostatic system should be independent from the detected electron energy, the above mentioned measurement and calculation method were also repeated at 50 eV and 804 eV primary electron energies on Kr and Ne targets for elastic electron scattering and at 1.9 keV primary electron energy for  $M_{45}N_{23}N_{23}$  and  $KL_{23}L_{23}$  Auger lines of Kr and Ne atoms, respectively. The derived angle dependent transmission functions agree very well with each other confirming the energy independence of the spectrometer transmission function. This means that the energy dependence of the relative efficiencies of the detectors can be obtained without the rotation of the detector holder, i.e. only the energy of the incident electron beam needs to be changed. As a result in [Fig. 5](#) the near isotropic transmission corrected elastic peak intensities show the relative efficiencies of the detectors without any normalization.

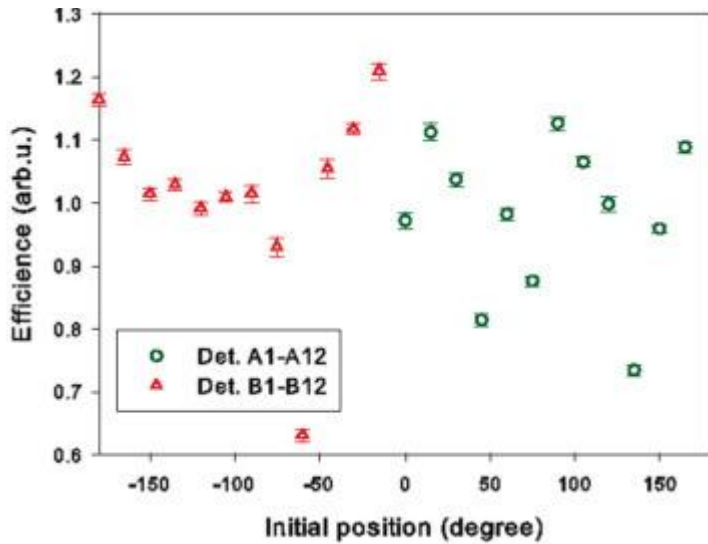


Fig. 6.

Relative efficiencies of the channeltrons as a function of the initial angular positions of the detectors (green open circles: A1=0°,A2=15°,... and B1=-15°,B2=-30°,...). The kinetic energy of the elastically scattered electrons was 205 eV. (For interpretation of the references to colour in this figure legend, the reader is referred to the web version of this article.)

[Figure options](#)

## 4. The absolute calibration method

The energy dependence of the absolute detector efficiencies ( $\eta(E)$ ) can be determined easily by means of the elastic electron scattering process and the experimentally obtained transmission function of the ESA-22 electron spectrometer. We assume that the energy dependence of the theoretical single differential elastic cross sections is well known and these values are realistic at the polar angle  $\theta=90^\circ$ . When Eq. (1) is applied for this process, only the energy dependence of the detector efficiencies ( $\eta(E)$ ) remains unknown. For a single angular channel it can be expressed as equation(8)

$$\eta(E) = \frac{I_d}{(d\sigma(E)/d\Omega)I_p n_t L T \Delta\Omega}.$$

[Turn MathJax on](#)

To get the energy dependent efficiencies ( $\eta$ ) differential elastic scattering cross sections were measured for electron impact on argon gas in the primary electron energy range of 50 eV and 2000 eV. NIST data base [12] was used as elastic cross section reference in Eq. (8). The experiments were performed with homogeneous argon gas target. The vacuum chamber was filled with argon gas up to the pressure  $1 \times 10^{-4}$  mbar (the background pressure without argon gas was  $5 \times 10^{-8}$  mbar). In the present geometry the target thickness  $L$  is independent from the observation angle and it is determined by the exit slit of the spherical mirror (its magnification is unity). The solid angle  $\Delta\Omega$  can be calculated from the entrance slit of the inner sphere and the dimensions of the detectors for a single angular channel. The electron current was measured with a digital current integrator ORTEC 439. Fig. 7 shows the absolute efficiencies for the 20 detectors as a function of the scattered electron energy. 4 CEMs were shaded by some parts of the spectrometer

during the data collection. The measurement was repeated one day later at several primary electron energies and the slight differences (maximum 6%, see [Fig. 7](#)) between the experimental data show the reproducibility of the gas pressure. Since our experimental data were compared with the cross sections from NIST data base [\[12\]](#), we could not fully satisfy the absolute calibration of a low energy electron spectrometer. But our calibration method can be suitably used in a wide energy range of the detected electrons in case of angular distribution measurements without absolute cross section values.

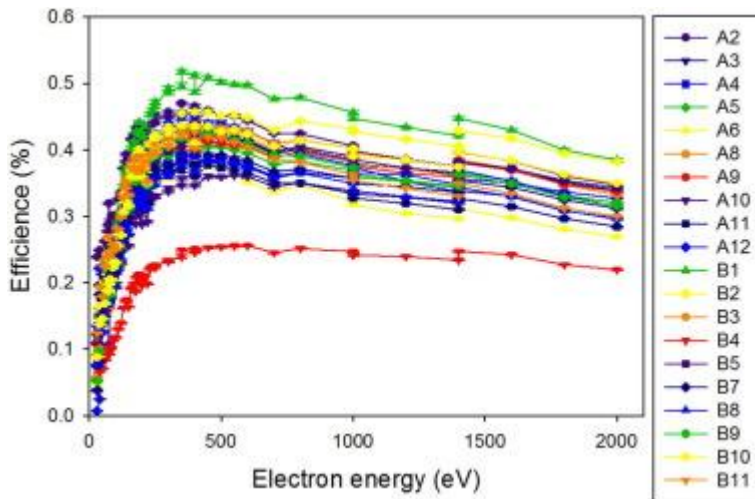


Fig. 7.

Absolute detector efficiencies (symbols connected with solid lines) as a function of the electron energy.

#### [Figure options](#)

As a test of this calibration method, in cooperation with the German National Metrology Institute (PTB), the double differential (in energy and angle, DDCS) ionization cross sections were measured for the collision of 300 keV protons with argon in the polar angular range ( $\psi$  in [Fig. 2a](#)) of  $\pm 15^\circ$  and  $\pm 165^\circ$  relative to the proton beam direction ( $X$  axis in [Fig. 2a](#)). The measuring geometry can be seen in [Fig. 2a](#). The experiments were carried out at the 3.75 MV Van de Graaff accelerator at PTB (Braunschweig, Germany). [Fig. 8](#) compares the present and the previous [\[1\]](#) experimental DDCS values at emission angles  $15^\circ$ ,  $75^\circ$  and  $165^\circ$  relative to the proton beam direction as a function of the electron energy. The good agreement between the two data sets shows that the presently developed method is suitable and reliable to calibrate an electron spectrometer.

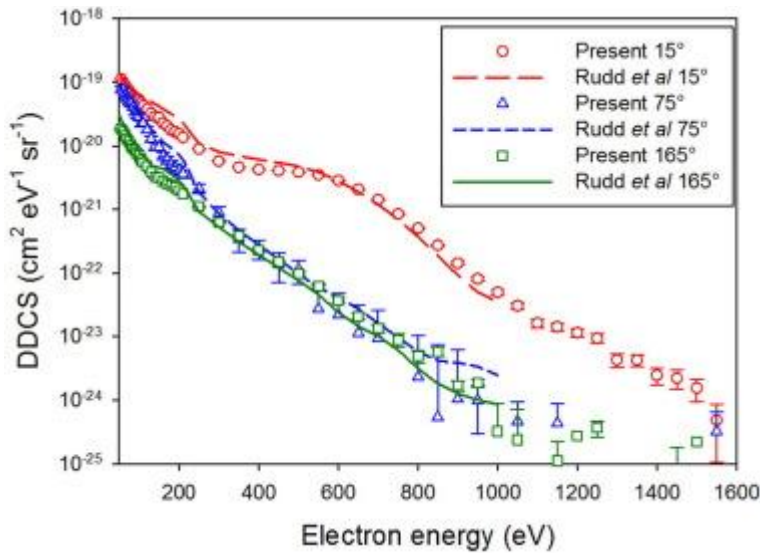


Fig. 8.

Experimental double differential ionization cross sections (DDCS) (symbols) for the ionization of argon by 300 keV protons in comparison with the results of Rudd et al. [1] (solid, short and medium dashed lines) at observation angles 15°, 75° and 165° ( $\psi$  in Fig. 2a) relative to the proton beam direction ( $X$  axis in Fig. 2a) as a function of the ejected electron energy.

[Figure options](#)

## 5. Conclusions

The recently upgraded ESA-22 electrostatic electron analyzer and a new calibration method for electron spectrometers were presented. An electron gun along the spectrometer axis and a rotatable detector holder around the axis of the cylindrical mirror were installed inside the analyzer. The transmission function of the spectrometer and the absolute and relative efficiencies of the individual detectors were determined by measuring the elastically scattered electrons. The calibration procedure was tested by measuring the double differential ionization cross sections (DDCS) for the ejection of secondary electrons by collision of 300 keV protons with argon. The experimental data were compared with the DDCS values published by Rudd et al. [1]. The good agreement between the two data sets verifies the applicability of the calibration method.